

ornl

ORNL/TM-10739

**OAK RIDGE
NATIONAL
LABORATORY**

MARTIN MARIETTA

**A Preliminary Assessment of the
Relationship Between the Mineralogy
and Diagenetic History of Four
Argillaceous Rocks and Their
Thermomechanical Properties**

Otto C. Kopp
Patrick J. Mulligan
Daniel K. Reeves

OAK RIDGE NATIONAL LABORATORY

CENTRAL RESEARCH LIBRARY

CIRCULATION SECTION

4500N ROOM 175

LIBRARY LOAN COPY

DO NOT TRANSFER TO ANOTHER PERSON

If you wish someone else to see this
report, send in name with report and
the library will arrange a loan.

UCN-7969 (3 9-77)

OPERATED BY
MARTIN MARIETTA ENERGY SYSTEMS, INC.
FOR THE UNITED STATES
DEPARTMENT OF ENERGY

Printed in the United States of America. Available from
National Technical Information Service
U.S. Department of Commerce
5285 Port Royal Road, Springfield, Virginia 22161
NTIS price codes—Printed Copy: A06 Microfiche A01

This report was prepared as an account of work sponsored by an agency of the United States Government. Neither the United States Government nor any agency thereof, nor any of their employees, makes any warranty, express or implied, or assumes any legal liability or responsibility for the accuracy, completeness, or usefulness of any information, apparatus, product, or process disclosed, or represents that its use would not infringe privately owned rights. Reference herein to any specific commercial product, process, or service by trade name, trademark, manufacturer, or otherwise, does not necessarily constitute or imply its endorsement, recommendation, or favoring by the United States Government or any agency thereof. The views and opinions of authors expressed herein do not necessarily state or reflect those of the United States Government or any agency thereof.

CHEMICAL TECHNOLOGY DIVISION

A PRELIMINARY ASSESSMENT OF THE RELATIONSHIP BETWEEN THE MINERALOGY
AND DIAGENETIC HISTORY OF FOUR ARGILLACEOUS ROCKS AND THEIR
THERMOMECHANICAL PROPERTIES

Otto C. Kopp
Patrick J. Mulligan
Daniel K. Reeves

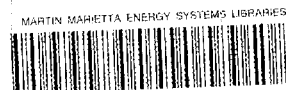
Department of Geological Sciences
University of Tennessee
Knoxville, Tennessee 37996-1410

Date of Issue -- November 1988

NOTICE: This document contains information of a preliminary nature.
It is subject to revision or correction and therefore does
not represent a final report.

Prepared for the
Office of Defense Waste and Environmental Restoration

Prepared by the
OAK RIDGE NATIONAL LABORATORY
Oak Ridge, Tennessee 37831
operated by
MARTIN MARIETTA ENERGY SYSTEMS, INC.
for the
U.S. DEPARTMENT OF ENERGY
under contract DE-AC05-84OR21400



3 4456 0283870 3

TABLE OF CONTENTS

	<u>Page</u>
LIST OF FIGURES	iv
LIST OF TABLES	v
ABSTRACT	1
1. INTRODUCTION	3
1.1 INTRODUCTION AND PURPOSE	3
1.2 PREVIOUS STUDIES	3
1.3 ACKNOWLEDGMENTS	5
2. METHODS	5
2.1 STANDARDS AND SAMPLES.	5
2.2 SPECIFIC GRAVITY	6
2.3 WATER CONTENT	10
2.4 X-RAY FLUORESCENCE ANALYSIS.	11
2.5 X-RAY DIFFRACTION ANALYSIS	12
2.5.1 Mineralogical Analysis.	12
2.5.2 Preferred Orientation (Fabric) Analysis Using XRD	14
2.6 SCANNING ELECTRON MICROSCOPY	15
3. RESULTS AND DISCUSSION.	16
3.1 SPECIFIC GRAVITIES	16
3.2 WATER CONTENT.	17
3.3 X-RAY FLUORESCENCE ANALYSES.	19
3.4 QUANTITATIVE MINERALOGICAL ANALYSES.	21
3.5 PREFERRED ORIENTATION ANALYSES USING XRD	29
3.6 RESULTS OF SEM ANALYSES.	34
4. FURTHER DISCUSSION AND CONCLUSIONS.	41
5. REFERENCES.	47
6. APPENDIXES.	49
Appendix A. Procedure for the Determination of Specific Gravities of Shales	51
Appendix B. The CLAYS Protocol	53
Appendix C. Chemical Compositions of Samples	57
Appendix D. Preparation of "L-Shaped" Blocks	61

LIST OF FIGURES

<u>Figure</u>		<u>Page</u>
1.	X-ray diffraction patterns of samples of Devonian Shale (DS1)	31
2.	X-ray diffraction patterns of samples of Pierre Shale (PS2)	32
3.	SEM photograph of a relatively large detrital muscovite (illite) grain	35
4.	SEM photograph of a silt-size, detrital quartz grain. .	37
5.	SEM photograph of a silt-size, detrital albite grain. .	38
6.	SEM photograph of clusters of framboidal (?) iron oxide grains	39
7.	SEM photograph of aragonite or fibrous calcite grains. .	40
8.	SEM photograph of framboidal and euhedral pyrite grains.	42
9.	SEM photograph of a relatively large, possibly wind-blown grain of biotite	43

LIST OF TABLES

<u>Table</u>		<u>Page</u>
1.	Standards used to establish relative intensity ratios	7
2.	Samples analyzed	8
3.	Specific-gravity determinations.	17
4.	Water contents	18
5.	Comparison of relative intensity ratios (RIRs)	24
6.	Mineral concentrations (wt %) for selected samples . .	25
7.	Results of preferred orientation study using X-ray diffraction	33

A PRELIMINARY ASSESSMENT OF THE RELATIONSHIP BETWEEN THE MINERALOGY
AND DIAGENETIC HISTORY OF FOUR SHALES AND THEIR
THERMOMECHANICAL PROPERTIES

Otto C. Kopp
Patrick J. Mulligan
Daniel K. Reeves

ABSTRACT

The chemical, hydrologic, mechanical, and thermal properties of argillaceous material will be important in the geological disposal of high-level radioactive wastes. These important properties are strongly influenced by the mineralogical composition and previous diagenetic history of the argillaceous material.

Although many argillaceous samples have been analyzed to determine one or more of their chemical, hydrological, mechanical, or thermal properties, quantitative mineralogical compositions are only rarely determined, and their diagenetic histories are assessed even less frequently. Mineralogical and diagenetic information could be quite useful in explaining how clay-rich materials behave. As more information becomes available, it may be possible to predict their suitability for geological disposal on the basis of mineralogical composition and previous diagenetic history.

A primary purpose of this study was to develop reproducible, quantitative methods to determine the bulk mineral composition and diagenetic history of argillaceous rocks and to attempt, in a preliminary way, to explain the thermomechanical behavior of several formations that were being measured by others.

This report presents the results of several methods of analysis [specific-gravity determinations, water contents, chemical analyses by X-ray fluorescence (XRF) analysis, quantitative mineralogical analyses by X-ray diffraction (QXRD), preferred orientation analyses by X-ray diffraction, and scanning electron microscopy (SEM) of fractured samples] that were used to study selected samples from the Conasauga Group, the Rhinestreet Shale, the Pierre Shale, and the Green River Formation to determine their mineralogical character and the effects of diagenesis on these materials. The results were then related to thermomechanical test data that were obtained on samples from the same cores.

Specific-gravity determinations on "as-received" samples ranged from 2.00 for the Green River Formation to 2.75 for the Rhinestreet Shale. Exposure to the atmosphere resulted in a small net gain (+0.5) in specific gravity for the Conasauga Group samples and a net loss (-0.11) for the Pierre Shale samples. Water contents, determined by heating to 105°C for 1 h, averaged 0.8% by weight for the Conasauga Shale, Rhinestreet Shale, and Green River Formation samples. The water content determined for the Pierre Shale samples was 12.1 wt %.

Mineral concentrations (in weight percent) were determined using a modified pressed pellet, "matrix-flushing," and relative intensity method. Smectite and mixed-layer clays ranged in concentration from "not detected" in the Green River Formation samples and a Conasauga Shale sample to 26 wt % in a Pierre Shale sample. Kaolinite ranged in concentration from "not detected" to 14 wt % in a Rhinestreet Shale sample. Illite ranged from "not detected" in a Conasauga Shale sample to 36 wt % in a Rhinestreet Shale sample. Mineralogically, the Pierre Shale samples and the Green River Formation samples are the most homogeneous, while the Conasauga Group samples are the most heterogeneous.

Preferred orientation of clay flakes was studied using XRD and oriented shale blocks. Semiquantitative data were obtained by comparing the intensities of the (001) peaks of illite and kaolinite with the intensity of their combined (020) peak. Comparison of the ratios determined for the Pierre Shale and Rhinestreet Shale samples suggests that the clay flakes in the Rhinestreet Shale samples are more perfectly aligned than those in the Pierre Shale samples. By way of comparison, point-load index anisotropies determined by others for the Chattanooga Shale (a Devonian shale, which is quite similar to the Rhinestreet Shale) and the Pierre Shale are 10.5 and 1.8, respectively. SEM analyses substantiate the high degree of preferred orientation of clay flakes in the Rhinestreet Shale.

Using SEM analysis, calcareous and siliceous cements (which increase the strength of sedimentary rocks) were readily identified in the Conasauga samples as were trace amounts of pyrite, iron oxides, and other minerals that were too low in concentration to be detected by X-ray diffraction (XRD). SEM analyses also made it possible to determine the location of individual phases (such as the calcareous and siliceous cements in the Conasauga Group samples and pore spaces in the Pierre Shale samples). The presence of aragonite (or fibrous calcite) and pyrite along bedding planes reveals passageways for migrating fluids. Grain size and shapes aid in the recognition of detrital grains of clays, quartz, and feldspars in all samples, as well as biotite of possible volcanic origin in a sample of the Pierre.

The relatively high ultimate strength of the Green River Formation (74.7 MPa), measured by others is due to the presence of >50 wt % carbonates, which act like cement and bind grains together. Conversely, the relatively low ultimate strength of the Pierre Shale (7.2 MPa) results from its high water content (12.1 wt %) and inferred porosity (~24%), as well as its high concentration (~25 wt %) of mixed-layer clays.

1. INTRODUCTION

1.1 INTRODUCTION AND PURPOSE

The technology development described in this report evaluates shales and other argillaceous material for the geological disposal of high-level radioactive wastes. A primary purpose of this study is to develop techniques for performing quantitative mineralogical analyses and assessing the effects of diagenesis. The initial mineralogical composition of sediments deposited in a basin and the changes that occurred as a result of diagenesis during burial can exert a strong influence on the chemical, hydrological, mechanical, physical, and thermal properties of sedimentary material.

Based on an extensive search of the literature (KOPP 1986), there appears to be a paucity of information concerning the mineralogy and diagenetic history of most argillaceous samples for which hydrological, mechanical, and thermal data have been obtained.

An attempt is made here to relate mineralogical compositions and diagenetic information to selected thermal and mechanical properties measured by HANSEN (1987). For this purpose, eight samples [two each from the Conasauga Group, the Rhinestreet Shale (Devonian), the Pierre Shale, and the Green River Formation] were selected for analysis. The results are discussed in this report.

1.2 PREVIOUS STUDIES

Several rock types, including both sedimentary and igneous rocks, have been considered as potential hosts for the geological disposal of radioactive waste. Among five sedimentary rocks that were considered (sandstone, shale, limestone-dolostone, anhydrite, and chalk), shales appear to have the best overall combination of properties for this purpose (CROFF, in preparation).

Shales and other clay-rich materials possess certain advantageous properties such as low hydraulic conductivity, adequate thermal conductivity, plasticity (which can aid in the self-healing of fractures), and good sorptive capacity (WEAVER 1976). However, all of these desirable properties may not be present. In addition, some

of these same desirable properties may be associated with other properties, such as low compressive strength and the tendency to creep. The effects of elevated temperatures (due to the thermal loading imposed by canisters that contain radioactive waste) on argillaceous materials are not thoroughly understood.

Shales and other argillaceous materials are mainly composed of clay minerals such as members of the illite, smectite (and clay-size vermiculite), kaolinite, and chlorite groups (SHAW 1965; POTTER 1980). Two or more clay minerals are usually present in a given sample and mixed-layer clays are common, especially in younger or less deeply buried formations. Clay minerals in the silt-size fraction may be important in determining the properties of argillaceous rocks. Other minerals, including quartz, calcite, dolomite, feldspars, pyrite, zeolites, various iron and aluminum oxides and oxyhydroxides, etc., may be present in amounts ranging from <1 to 50% by weight.

MEYER (1983) compares several properties (e.g., hydraulic conductivity, sorptive capacity, volume swell capacity, and shear strength) for clay species such as illite, kaolinite, and smectite and their admixtures with water, quartz sand, and other materials. RIEKE (1974) provides comprehensive data concerning the changes in hydrological, mechanical, physical, and thermal properties that take place as argillaceous sediments are buried. Many reports, proceedings, and papers discuss mineralogical changes that take place during the burial of argillaceous sediments. Even so, most of the available literature does not address the relationships between mineralogical composition, diagenetic history, and the properties that will determine whether a specific material is suitable for use in the geological disposal of high-level radioactive waste.

DELAGUNA (1968) provides adequate mineralogical data and other information on permeability and ion-exchange capacity to demonstrate the influence of mineral composition on these properties (KOPP 1987). More recently, HANSEN (1987) provides the results of

specific thermomechanical tests (unconfined compression, indirect tension, point-load index, creep, slake durability, and swell tests) for selected samples of the Pierre Shale, Green River Formation, Rhinestreet Shale, Carlile Shale, and Chattanooga Shale. The Hansen report includes quantitative mineralogical compositions for eight samples of the Pierre Shale, and one sample each of the Carlile Shale, Conasauga Group, Chattanooga Shale, Green River Formation and Rhinestreet Shale. The mineralogical analyses were performed by B. L. Davis, Institute of Atmospheric Sciences, South Dakota School of Mines and Technology, Rapid City, South Dakota, using thin-layer aerosol samples (DAVIS 1982 and 1984). Davis' method and results will be compared with the method and results described in this report.

A more complete discussion of previous attempts to obtain QXRD analysis and a statistical evaluation of the methods used to prepare and analyze the samples in this study are given by MULLIGAN (1987).

1.3 ACKNOWLEDGMENTS

Several persons contributed to this report. We are especially grateful to Thomas F. Lomenick and Thomas W. Hodge, Jr., of the Chemical Technology Division, Oak Ridge National Laboratory (ORNL) for their assistance in providing samples and other technical support. Bill Leslie, of the Metals and Ceramics Division, ORNL, was most helpful during the analysis of several fractured blocks using SEM. We appreciate the helpful reviews provided by Richard Ketelle, Arlo Fossum, Serge Gonzales, and S. Y. Lee.

Finally, gratitude is expressed to Ms. Carol Proaps and Ms. Vicki Hinkel, Chemical Technology Division, ORNL, for their diligent secretarial and editorial assistance.

2. METHODS

2.1 STANDARDS AND SAMPLES

In order to perform the QXRD analyses discussed, it was necessary to use a number of mineral standards. Most of the clay mineral standards were purchased from the Clay Mineral Society.

The other minerals used for reference patterns came from the collections in the Department of Geological Sciences or were purchased from Ward's National Science Establishment in Rochester, New York. A list of the standards used in this study is given in Table 1. Note that completely pure minerals are the exception rather than the rule. Each mineral was analyzed using XRD to confirm its identity and to determine whether any impurities were present. This information is given in MULLIGAN (1987).

The sedimentary rock samples, which were analyzed by QXRD and other techniques described below, were supplied by T. W. Hodge, Jr. (ORNL). Offcuts of the samples analyzed by HANSEN (1987) were not available; however, eight samples were selected for analyses from the available core at ORNL. The samples are listed in Table 2 with brief descriptions of their physical characteristics.

2.2 SPECIFIC GRAVITY

Specific gravity is a dimensionless quantity that gives the density of a substance relative to the density of pure water at a specified temperature, usually 20°C (although other temperatures may be used). Since the density of water at 20°C is 0.998 g/cm³, densities measured in grams per cubic centimeter at 20°C for most substances can be converted directly to specific gravities without introducing any significant errors. (Note: numerically, values of specific gravity are equal to densities measured in grams per cubic centimeter.)

Specific gravities can be determined for several kinds of samples, depending on the material available and the information sought: "as-received," "air-dried," "oven-dried" (at a specified temperature); and even the specific gravities of the grains can be determined. In this study, the as-received and air-dried specific gravities of bulk samples are of interest because these values may provide information related to the mineralogical and/or chemical composition, the extent of compaction, and the extent to which pores are vacant, filled with fluids, or filled with mineral matter.

The specific gravities of coherent rocks with low porosities can be determined using the same techniques as for other solids; however, clays and shales may require special handling because of their fragile

Table 1. Standards used to establish relative intensity ratios

Clay Mineral Society Standards

IMt-1	Illite, Montana
KGa-1	Kaolinite, Georgia (well crystallized)
KGa-2	Kaolinite, Georgia (poorly crystallized)
NG-1	Nontronite, Germany
SCa-2	Smectite, California
SWa-1	Smectite, Washington
SWy-1	Smectite, Wyoming

Non-clay Minerals

Albite	Keystone, South Dakota
Aragonite	Somerset, England
Calcite	Chihuahua, Mexico
Calcite	Location unknown
Dolomite	Sussex, New Jersey
Pyrite	Location not known
Quartz	Brazil
Quartz	Location not known

Note: Standards were not available for chlorite, mixed-layer clays, and uncommon minerals such as dawsonite.

Table 2. Samples analyzed

ORNL identification	Our ID number	Description
Conasauga Group Bear Creek Valley ORNL, GW-137 (513.5 to 514.0 ft)	CS1	Highly variable shale, silty and calcareous; light gray (N7) to medium; dark gray (N4); wavy to irregular bedding, not obvious upon breaking.
Conasauga Group Bear Creek Valley ORNL, GW-139 (725 to 725.9 ft)	CS2	Shale, dark gray; part nodular, light gray (N7); in part, finely laminated; shale-rich portions contain micaceous material; some fracture porosity.
Devonian Shale (Rhinestreet Shale) West Virginia DR/86/181 (5256 ft)	DS1	Very fine-grained shale; olive black (5Y2/1); very fine parallel laminations with minor silt; rich in organic matter.
Devonian Shale (Rhinestreet Shale) West Virginia DR/86/262 (5231 ft)	DS2	Very fine-grained, laminated shale with numerous silt particles; medium gray (N3); rich in organic matter.
Pierre Shale Mobridge Member DH-84-20(U14) (312.3 to 312.8 ft)	PS1	Very fine-grained shale; no obvious laminations; olive black (5Y2/1) to brownish black (5YR2/1); contains silt-size grains and micaceous flakes.
Pierre Shale Mobridge Member DH-84-20(U14) (314.4 to 314.9 ft)	PS2	Silty shale with no obvious laminations; medium dark gray (N4), but variable in color; easily broken with conchoidal fracture.

Table 2
(continued)

ORNL identification	Our ID number	Description
Green River Fm. Parachute, CO GR/86/V17-0 (11.79 to 12 ft)	GR1	Finely laminated and color-banded marlstone (?); grayish brown (5YR3/2) to medium brown (5YR3/4); relatively homogeneous, but contains fine-grained drusy crystals along lamination surfaces and coarser crystals along cleavage surfaces.
Green River Fm. Parachute, CO GR/86/V17-0 (12.5 to 12.75 ft)	GR2	Finely laminated and color-banded marlstone (?); with pods of organic debris; fairly homogeneous; grayish brown (5YR3/2) to dusky brown (5YR2/2); contains drusy crystals along fractures.

character and tendency to slake when immersed in water. In order to overcome these problems, each sample was coated with paraffin before immersion in water to determine its volume. The procedure is described in Appendix A.

2.3 WATER CONTENT

Determination of the water content is a relatively simple procedure. A small quantity of the sample (usually 5 to 10 g), which has been crushed to "pea" size (approximately 2 to 5 mm in diameter), is weighed to the nearest 0.01 g in a beaker of known weight. In an attempt to remove only the pore water, the sample is heated in an oven at 105°C for 1 h, removed, and reweighed. Some workers prefer to heat the sample for 24 h at 105°C; however, extended heating may also drive water out of interlayer sites. The water content is calculated from the weight loss during this procedure.

There are several problems with this determination. If the sample has been exposed (air dried) for any length of time, it may have already lost part (or nearly all) of the moisture contained in its pores, depending on the sizes of the pores and the degree to which they are interconnected. Clay-rich samples are more difficult to work with because some clay minerals (especially smectites, vermiculites, and mixed-layer clays) may hold a significant fraction of the water contained in the sample in interlayer sites (within the clay flakes) rather than in intergranular pore spaces. The amount of water released from such sites, after heating for the prescribed time at 105°C, is affected by factors such as the size of the clay grains, their mineralogical composition, and the nature of the ions in the interlayer sites. Even so, the determination is worth the small effort involved. Samples that have been air dried typically show little weight loss, as do the samples that have been thoroughly compacted as a result of deep burial or having been extensively cemented. On the other hand, geologically younger formations that were never deeply buried may contain >25% water by weight.

The amount of water lost during heating may yield some preliminary information concerning the amount of pore space in the sample and may provide clues to the relative strength of the material during handling and excavation or the possible release of water during the thermal loading, which would be imposed by nearby radioactive cannisters.

2.4 X-RAY FLUORESCENCE ANALYSIS

XRF analysis is a nondestructive X-ray method for determining the chemical composition of a wide range of materials. Each sample, which was previously air dried at 105°C for 1 h, is irradiated with a beam of primary X-rays, producing a spectrum of secondary X-rays. The spectrum of secondary X-rays is recorded and analyzed to determine the elements present in the sample and their concentrations in weight percent. The method is relatively rapid (as many as 24 samples and/or standards can be analyzed overnight) and gives reproducible results (each time samples are analyzed, 3 or 4 standards are analyzed as unknowns and the results checked against their known compositions). Elements lighter than sodium cannot be analyzed directly.

In combination with XRD analysis, certain chemical elements can be related to the minerals that are present. For example, the common minerals in shales that contain potassium are K-feldspars, micas, and members of the illite and vermiculite groups. In many geologically older shales, the dominant mineral is illite and the amount of this clay present is closely related to the amount of K₂O present in the sample analyzed. Large concentrations of CaO are most likely due to calcite, aragonite, or dolomite, although some may be present in smectites. The analytical program calculates the sum of the weight percents of all the elements analyzed, providing a clue to the quantity of any material that was not analyzed (e.g., discrete water, carbon dioxide, and organics).

In the present study, no attempt was made to determine the sorption characteristics of the samples. This is best done by determining sorption coefficients (K_{ds} or R_{ds}); however, XRF can be used to estimate the cation- and anion-exchange capacities of clays,

shales, soils, and similar geological material, using barium chloride. The procedures are described by MONGER (1986).

2.5 X-RAY DIFFRACTION ANALYSIS

XRD has been one of the most widely used methods of mineral identification since the 1930s. It is especially valuable in the identification of clay minerals because their fine grain size and lack of distinctive physical properties make it virtually impossible to distinguish these minerals in hand specimens. The basic technique is so familiar that no attempt will be made to describe the method in this report.

XRD was the primary analytical method used to determine the minerals present in the ORNL samples analyzed in this study. The mineralogical analyses were performed on bulk samples (pack mounts); pressed pellets; pressed pellets with Linde C corundum (1 μm , nominal; alpha form, 99.98% purity; Union Carbide Corporation, Coatings Service Dept., 1550 Polco St., Indianapolis, IN 46224) as an internal standard; pressed pellets with Linde C corundum internal standard, which were spiked with known quantities of quartz, calcite, or dolomite; and elutriated slides (prepared by settling samples from water suspensions onto glass slides). In addition, cut blocks of representative shale samples were used for preferred orientation (fabric) analysis using XRD.

2.5.1 Mineralogical Analysis

MULLIGAN (1987) provides a detailed discussion of the development of QXRD and describes the methods used for analyzing the samples listed in Table 2, Section 2.1. The method involves several forms of analysis. A hand-ground, pack-mount sample was analyzed initially to determine the mineral phases present and the positions of their most intense peaks. Relative intensity ratios (RIRs) were determined using pressed pellets prepared from 3.000 g of sample and 1.000 g of Linde C corundum. As originally proposed, RIR, the ratio of the most intense peak of a mineral to the intensity of the most intense peak of corundum, was determined using a sample containing equal amounts of the mineral and corundum (a 50:50 ratio by weight). We found that

using a 75:25 ratio of sample to corundum increased the intensities for the mineral peaks, while still providing adequate intensities for the strongest corundum peak at 0.2085 nm. RIR values for several minerals are compared in Section 3.4.

A second pellet of each sample was prepared using quartz as a spike in the following proportions: Linde C corundum, 1.000 g (25%); quartz, 0.800 g (20%); and the sample, 2.200 g (55%). In addition, calcite was added as a spike to samples CS1, CS2, PS1, and PS2, and dolomite was added as a spike to samples GR1 and GR2 in the same proportions. These spiked samples were used to estimate the concentrations of quartz and/or calcite and dolomite in each of the samples through linear regression analysis (MULLIGAN 1987).

Pellets are prepared from previously ground powders, which are carefully mixed and ground together (using Freon as a grinding aid) in a Shatterbox and pressed at 207 MPa (30,000 psi). The sample plus corundum pellets are used to determine RIRs for the mineral phases present. This information is used to calculate the quantities of each mineral phase present using the method of CHUNG (1974a and 1974b). DAVIS (1982 and 1984) uses a similar method (the relative intensity method, RIM) in which unoriented samples obtained by trapping spray-dried powders on fiberglass filters are X-rayed. A major advantage of Davis' method is the ability to calculate the amount of amorphous material present using X-ray absorption. Davis' technique, however, has some disadvantages: the unoriented, spray-dried samples have very low packing densities, reducing diffraction intensities, and correction factors must be applied to compensate for the different amounts of powder trapped each time a new sample is prepared. The technique described by MULLIGAN (1987) cannot be used in its present form to determine with assurance the amount of amorphous material present.

In addition to the bulk and pressed pellet samples, elutriated slides were also X-rayed. These samples are enriched in the clay-size fraction and are more highly oriented than pressed pellets. The clay mineral phases can be further analyzed and subjected to both glycolation and heat treatment to distinguish minor amounts of

individual clay mineral species present. Elutriated slides are essential for distinguishing certain clay minerals, such as chlorite. Perhaps the greatest difficulty in using RIR-based methods of QXRD is that clay minerals vary so much in their degree of crystallinity and chemical composition (mixed-layer clays and solid solutions are very common). In most analyses, an RIR value is assigned to each mineral phase, and that value is used to calculate the quantity of each mineral present. However, the present study has shown that RIRs for individual specimens within a group (such as the smectite group) may vary by a factor of 5 to 6 times (e.g., for four smectite standards, the RIRs ranged from 1.4 to 8.1). The lack of representative standards for some minerals (e.g., clay-size chlorite, clay-size vermiculite, and dawsonite) made it impossible to determine their RIRs. The concentration values for chlorite were determined using the method of GRIFFIN (1970). No attempt was made to quantify dawsonite.

No attempt was made in this study to determine the lower limits of detection for individual minerals. PAWLOWSKI (1987) determined lower limits of detection for several phases: 0.5% for quartz, calcite, and dolomite; 7% for illite; and 40% for glass.

2.5.2 Preferred Orientation (Fabric) Analysis Using XRD

In several previous reports (summarized by KOPP 1986), shale properties, such as mechanical strength, hydraulic conductivity and thermal conductivity, are shown to vary with test direction (i.e., whether the property is measured parallel to or perpendicular to the bedding). The reported values may differ by more than an order of magnitude. HANSEN (1987) reports the average point-load index for Pierre Shale perpendicular to bedding as 0.27 MPa and parallel to bedding as 0.13 MPa, giving the index an "anisotropy" of two. For samples of the Chattanooga Shale, the average index strength parallel to bedding is 0.32 MPa, while the average index strength perpendicular to bedding is 3.37 MPa, giving the index an anisotropy of 10.5.

Several factors, primarily the degree of preferred orientation of the clay grains (but also other factors such as the degree of

cementation) may be responsible for the differences in shale properties with direction. In order to determine any such relationships, several samples were cut into "L-shaped" blocks, one leg of which is essentially parallel to the bedding and the other is essentially perpendicular to the bedding. The procedures for cutting the blocks are described in Appendix D.

Each leg of the L-shaped block was X-rayed, one parallel to the bedding and the other perpendicular to the bedding. The XRD patterns were measured and the intensities of two (or more) clay peaks with known crystallographic orientations parallel to the basal planes (the 001 planes) and at a high angle to the basal plane (such as the 020 planes) were determined. Intensity ratios were calculated for the "parallel-to-bedding" and "perpendicular-to-bedding" orientations and compared with each other. The results suggest that XRD of oriented blocks can provide semiquantitative information concerning the degree of preferred orientation of the clay grains in a clay-rich rock. This information may be useful in predicting the degree of variation of certain mechanical, hydrologic, or thermal properties with direction.

2.6 SCANNING ELECTRON MICROSCOPY

SEM makes it possible to magnify images of surfaces up to 100,000X or more, although for most purposes, lower magnifications suffice. Fractured blocks from each sample were prepared and carbon coated to provide adequate electrical conductivity. Details of the method are given by MULLIGAN (1987). Semiquantitative chemical analyses (sodium is the lightest element that can be detected) can be obtained readily for selected grains or surface areas. If desired, quantitative analytical data can be obtained, but this procedure requires much more time. Since one of the goals of this study was to examine the changes that occur during diagenesis (such as reorientation of grains, recrystallization, and cementation), a decision was made to use most of the available instrumental time for

the examination of diagenetic features, and only rapid, semiquantitative chemical analyses were made of selected grains.

Tentative identification of individual mineral grains was based on available information, including the size and shape of the grain, the major elements present (using semiquantitative analysis), and prior knowledge of the bulk mineralogy of the rock obtained using XRD. Examples are given in the Results and Discussion section, and additional examples are described by MULLIGAN (1987).

3. RESULTS AND DISCUSSION

3.1 SPECIFIC GRAVITIES

Specific gravities were determined for representative bulk samples from each of the eight cores selected for analysis. The specific gravities were measured twice. The first determination was made on material that was kept in sealed plastic bags while the samples were being divided for the several analyses performed in this study. The second determination was made on samples that had been exposed to the atmosphere for a period of 1.47×10^6 s (17 d). Although it was not anticipated that the effects of exposure to air would go to completion in this brief time, the results of the second determination are compared with the results of the first determination to reveal the general effects of exposure on representative shale samples.

Note that only the Pierre Shale cores had been stored in containers sealed with wax that would reduce the evaporative loss of water. It was expected that changes in specific gravity as a result of moisture loss (or gain) for samples CS1, CS2, DS1, DS2, GR1, and GR2 would be minimal because these samples had been buried more deeply and subjected to more compaction, reducing the amount of pore space present. The data are given in Table 3. Specific-gravity changes less than ± 0.02 are probably not significant, but larger changes are thought to result from actual changes in the moisture content of the samples exposed to air. Neither the Rhinestreet Shale samples (DS1 and DS2) nor the Green River Formation samples (GR1 and GR2) reveal

Table 3. Specific-gravity determinations

Sample	Specific gravity (as received)	Specific gravity (air dried)	Change
CS1	2.73	2.77	+0.04
CS2	2.71	2.77	+0.06
DS1	2.75	2.75	0.00
DS2	2.74	2.76	+0.02
PS1	2.13	2.00	-0.13
PS2	2.11	2.02	-0.09
GR1	2.02	2.02	0.00
GR2	1.97	1.96	-0.01

any significant changes in specific gravity. The mineralogical (and organic) components of the Green River Formation are relatively free from smectites, mixed-layer clay, or other compounds that might easily lose or gain moisture from the atmosphere.

The Conasauga Group samples (CS1 and CS2) show an average specific-gravity gain of +0.05. It is possible that the two samples selected for air-dried determination had slightly higher specific gravities than the two chosen for the as-received determination; however, the specific gravities of both samples increased during exposure, and their net changes in specific gravity (+0.04 and +0.06) are very similar. It is possible that the gain in moisture content during exposure to the atmosphere was real. XRD analysis of sample CS2 reveals the possible presence of mixed-layer illite/smectite or hydrated micas.

The greatest changes in specific gravity were noted for the Pierre Shale samples (PS1 and PS2), which changed -0.13 and -0.09, respectively, because of moisture loss.

3.2 WATER CONTENT

The results of the water content determinations (based on weight-loss measurements at 105°C) are given in Table 4.

Table 4. Water Contents

Sample	Weight percent water (loss at 105°C)
CS1	0.6
CS2	0.9
DS1	1.4
DS2	0.9
PS1	12.1
PS2	12.1
GR1	0.6
GR2	0.6

The mean (\bar{x}) loss of water for six of the samples (CS1, CS2, DS1, DS2, GR1, and GR2) is 0.8% by weight and the standard deviation ($S\bar{x}$) is 0.3, suggesting that even these air-dried samples still retained small amounts of pore water and/or released small amounts of interlayer water held by minor amounts of smectites present. HANSEN (1987) reports average initial water contents for the Rhinestreet Shale and Green River Formation as 1.5 and 0.5%, respectively. These values are in good agreement with the data reported in Table 4.

The water loss determined for the Pierre Shale samples (PS1 and PS2) is much greater (average water content = 12.1 wt %). The presence of water may be an important factor in considering any geological material for use as a host repository. HANSEN (1987) reports initial water contents for several members of the Pierre Shale (based on samples of unknown size heated at 105°C for 24 h), ranging from 12.4 to 22.3%. Based on the relatively high pore water content, it may be inferred that the Pierre Shale is relatively weak mechanically. The Pierre Shale will be subject to changes in water

content and may shrink or swell, depending on temperature, humidity, and ionic environment or cation saturation conditions. The effects of thermal loading on expandable clay minerals as a result of emplaced waste canisters will need to be investigated because pore fluids and water contained in the interlayer site are likely to be released when they are heated.

If the specific gravity of the air-dried bulk Pierre Shale samples tested is approximately 2.0 and an assumption is made that all of the water released at 105°C (1 h) filled the available pore space, then a sample containing 12 wt % water would have a porosity of approximately 24%, and a sample containing about 22 wt % water would have a porosity of approximately 44%. Note that according to BURST (1969), porosities >50% are known to occur only in muds very close to the sediment-water interface. The amount of pore water generally decreases to <30% by the time the specific gravity of a mud has increased to 2.0. Based on the initial water contents determined by HANSEN (1987), it appears that some of the water released during heating at 105°C must have come from the interlayer sites in clay minerals. Therefore, "initial" water contents cannot be used with certainty to determine absolute values of porosity. Based on the relatively large water loss during heating and weight losses that occur when samples of the Pierre Shale are exposed to the atmosphere (Table 3, Section 3.1), it appears that the Pierre Shale has significantly greater effective porosity than the other samples analyzed.

3.3 X-RAY FLUORESCENCE ANALYSES

Samples of CS1, CS2, DS1, DS2, PS1, PS2, GR1, and GR2 air dried at 105°C for 1 h were analyzed chemically using an EG&G ORTEC Tube-Excited Fluorescence Analyzer. Information concerning the analysis is presented in Appendix B.

The results of the analyses are presented in Appendix C. One of the standards that was analyzed as an unknown (Appendix B, Table B.3, Sample: SGRI) is a U. S. Geological Survey standard from the Green River Formation. Appendix C also includes a sample of Chattanooga Shale (CHAT1) for comparison with the Rhinestreet Shale samples (DS1

and DS2). Typical analytical precisions or standard errors of calibration (see Table B.2, Appendix B) range from 0.05% for K_2O to 0.29% for SiO_2 (one standard deviation) for major elements.

Comparison of the analyses for the eight samples presented in Appendix C reveals some distinct chemical signatures that result from differences of the mineralogical compositions of the four formations analyzed. The Conasauga Group samples (CS1 and CS2) contain large amounts of CaO (14.78 and 10.53%, respectively) because of the relatively large amounts of calcite present in these samples. Na_2O concentrations are 2.00 and 2.15%, and K_2O concentrations are 1.91 and 3.00%, respectively. These alkalis may be contained within the mixed-layer, illite-smectite clays and feldspars revealed by analysis of other samples analyzed by XRD. The distribution of calcite, quartz, and the clay minerals in the Conasauga Group samples is not uniform. The total calculated value is 79.21% for CS1 and 87.97% for CS2.

The Rhinestreet Shales (DS1 and DS2) are characterized by higher concentrations of K_2O (4.62 and 4.63%), lower concentrations of Na_2O , and higher concentrations of Al_2O_3 relative to the concentrations of SiO_2 , which is typical of illite-rich samples. CaO concentrations are only 0.26 and 0.36% because of the general absence of carbonate grains or cement in these samples. Iron (expressed in terms of Fe_2O_3) is present in greater amounts than in the Conasauga Group samples, and the sulfur concentration in DS1 is 1.86%. Iron and sulfur occur in pyrite, which was detected in the SEM analyses but not in the XRD patterns. The presence of abundant pyrite, as well as organic material (which could not be detected by either the XRF or the XRD methods used), will help to maintain reducing conditions in an aqueous environment. Note that the total calculated values (100.41 and 96.88%, respectively) are thought to be a result of the near-total absence of carbonates. Chemical analysis of the Chattanooga Shale (CHAT1) sample reveals that it is rich in iron (9.96%) and sulfur (8.80%) in pyrite and sulfur-bearing organics. This sample of the Chattanooga Shale may be richer in organics (its total calculated value is only 84.07%) than the Rhinestreet Shale (DS1 and DS2).

The Pierre Shale (PS1 and PS2) contains higher concentrations of Fe_2O_3 (6.95 and 5.71%) and S (1.07 and 2.08%) due, in part, to the presence of pyrite but lower concentrations of K_2O (2.39 and 2.17%) than the Rhinestreet Shale (4.62 and 4.63%). The relatively high concentrations of CaO (6.50 and 6.29%) are the result of the presence of calcareous and apatite-bearing fossils, as well as other carbonate grains. The total calculated values (84.14 and 85.68%) are lower than those of the Rhinestreet Shale, which is thought to result from the larger amounts of carbonates and mixed-layer (and/or smectitic) clays present in the Pierre Shale.

The Green River Formation samples (GR1 and GR2) show the lowest total calculated values of any of the eight samples analyzed (59.67 and 55.63%) because of the large quantities of carbonates and organic compounds present. The U.S. Geological Survey standard, SGR1, (Appendix B, Table B.5) gives a total calculated value of 57.75%, which agrees closely with the total calculated values obtained for samples GR1 and GR2. Both Green River Formation samples are relatively low in K_2O (1.10 and 0.85%) and Fe_2O_3 (1.97 and 2.26%) and relatively high in CaO (17.48 and 9.98%) and MgO (4.74 and 4.55%) compared with most of the other samples analyzed, except for CS1 and CS2, which also contain high concentrations of CaO. XRD analyses of the Green River Formation samples reveal the presence of both calcite and dolomite.

3.4 QUANTITATIVE MINERALOGICAL ANALYSES

An initial goal was to devise a QXRD method, using counting rates determined by accumulating 10,000 counts (1% relative error) or a maximum counting time of 100 s for minor phases. The initial determinations of linear least-squares fits using quartz spikes were very successful and lead to the conclusions (MULLIGAN 1987) that it is possible to: (1) prepare pellets that are statistically uniform in composition; (2) prepare replicate pellets from the same starting materials; (3) correct counting rates for different clay-mineral matrices (kaolinite, illite, and smectite) using an internal standard

(Linde C corundum powder); and (4) use the linear relationship between counting rate and concentration to calculate concentrations from RIRs.

When all of the analytical data were collected and reduced using the method by CHUNG (1974a and 1974b), there were two major problems. First, the diffractometer used in this study was not computer controlled and could not collect counts for fixed time intervals over predetermined 2θ intervals. Instead, it was necessary to use the largest available receiving slit (nominally, 4° , but the actual subtended angle is only 0.6°) and manually set the position of the detector to receive the greatest counting rate for each individual peak. This meant that very narrow, well-defined peaks included background counts from their flanks, while for very broad peaks, many of the counts fell outside the angular range of the receiving slit and were lost. The differences in the widths of peaks generated by well-crystallized minerals (such as quartz and kaolinite) and poorly crystallized minerals (such as some smectites and mixed-layer clays) were beyond our ability to correct. The second major problem could affect the results not just of this study but work done by Davis or any other researchers using QXRD. It is concerned with the calculation of the RIR constants relating counting rates and concentrations of phases in a mixture. RIRs for different specimens of the same mineral standards might differ by more than an order of magnitude, as in the case of some smectites. Even for better crystallized clay minerals (such as the kaolinites), RIRs might differ by a factor of 2.

To overcome the first difficulty, previously run XRD patterns of pressed pellets (used to identify the phases present and to determine the positions of peaks and background used to take counts) were reexamined. The areas under the peaks of interest were measured by the triangle method (i.e., multiplying the peak heights by their widths at half their height). These peak areas were used to assess the relationship between total counts and mineral phase concentrations. The results looked promising, so the peak areas were measured again using a Numonics Model 1224 electronic digitizer, which gave even better results.

The RIRs determined initially by counting, those determined by using the triangle method, and those obtained using the electronic digitizer, are compared in Table 5, which also includes the RIR values of DAVIS (1984) and PAWLOWSKI (1985), as reported by DAVIS (1987). Note the wide range of RIR values. Of course, individual researchers would use their own RIR values that had been determined from standards prepared in a specific manner, using standard instrumental settings, etc. Still, under carefully controlled conditions, different values were obtained for some minerals (e.g., 6.9 and 8.6 for two kaolinites; 1.4, 4.4, 5.6 and 8.1 for four smectites). When two or more RIR values were available, they were averaged before being used to calculate concentrations.

The mineral concentrations were calculated using Chung's method (CHUNG 1974a and 1974b) and the equation:

$$[X_i] = \frac{1}{1 + K_i/I_i \sum_{i=1}^n I_i/K_i \dots\dots\dots I_n/K_n} ,$$

where

- $[X_i]$ = the concentration of the phase in the sample, and
- K_i = the reciprocal of RIR (CHUNG 1974a) determined as:

$$K_i = \frac{[X] \text{ standard}}{[X_i]} \cdot \frac{I_i}{I \text{ standard}}$$

where

I_i = intensity of mineral peak.

Table 6 reports the concentrations of the minerals identified in samples CS1, CS2, DS1, DS2, PS1, PS2, GR1, and GR2 and compares these values with the concentrations reported by HANSEN (1987) for samples

Table 5. Comparison of relative intensity ratios (RIRs)

Mineral	Relative intensity ratios				
	Counting ^a	Triangle ^b	Digital ^c	Davis ^d	Pawlowski ^e
Albite	2.9	3.6	3.9	1.5-2.1	9.0
Aragonite	0.7	1.7	1.4	-	-
Calcite	2.0; 3.1	3.8; 3.9	3.6; 3.8	6.0	17.4
Dolomite	2.0	4.3	4.4	4.2	32.4
Illite	2.5	6.2	4.7	1.8	0.4
Kaolinite ^f	4.9; 8.5	6.5; 11.2	6.9; 8.6	2.4	1.2
Pyrite	6.4	6.8	7.3	-	-
Quartz ^f	10.14; 12.3	1.5; 2.1 ^g	2.1; 2.5 ^g	8.4	11.4
Smectite ^h	0.1; 0.3; 1.0; 1.3	1.4; 5.5; 6.0; 10.5	1.4; 4.4; 5.6; 8.1	1.5	0.5

^aBased on counting rates using a nominal 4° receiving slit.

^bBased on peak areas using the triangle method.

^cBased on peak areas using Numonic digitizer.

^dDAVIS (1987); corrected to 3:1 ratio of sample to corundum.

^ePAWLOWSKI (1985); corrected to 3:1 ratio of sample to corundum.

^fTwo different standards used. Average RIR was used in calculating mineral concentrations.

^gThe 0.427 nm peak was used. The 0.334 nm peak was off the chart and its area could not be measured.

^hFour different standards used. The average RIR was used for calculating mineral concentrations.

Table 6. Mineral concentrations (wt %) for selected samples

Conasauga Group	CS1	CS2	Hansen ^a
Albite	22	13	(24.0) ^b
Calcite	31	35	(0.0) ^d
Chlorite	- ^c	9	20.4
Dolomite	-	-	(0.0) ^d
Illite	-	11	53.4
Kaolinite	2	5	0.0
Pyrite	-	-	2.2
Quartz	45	19	(24.0) ^b
M/L clays ^e	-	8	0.0
<hr/>			
Devonian shale	DS1	DS2	Hansen
Albite	7	10	(20.6) ^b
Calcite	-	-	(25.4) ^d
Chlorite	9	13	20.1
Dolomite	-	-	(25.4) ^d
Illite	36	12	31.0
Kaolinite	14	7	0.0
Pyrite	-	-	0.4
Quartz	28	51	(20.6) ^b
M/L clays ^e	6	7	0.0
<hr/>			
Pierre Shale (Mobridge Member)	PS1	PS2	Hansen ^f
Albite	9	6	(14.6-32.9) ^b
Aragonite	7	7	(19.1-56.5) ^d
Calcite	23	24	(19.1-56.5) ^d
Chlorite	- ^c	-	0.0-2.3
Dolomite	-	-	(19.1-56.5) ^d
Illite	14	13	3.5-13.6
Kaolinite	3	4	1.9-8.7
Pyrite	2	1	0.6-1.1
Quartz	18	20	(14.6-32.9) ^b
M/L clays ^e	26	24	13.1-25.1

Table 6
(continued)

Green River Formation	GR1	GR2	Hansen ^a
Albite	9	12	(31.3) ^b
Calcite	14	13	(50.5) ^d
Chlorite	- ^c	-	0.0
Dolomite	59	56	(50.5) ^d
Illite	2	3	3.9
Kaolinite	-	-	0.0
Pyrite	-	-	0.0
Quartz	16	16	(31.3) ^b
M/L clays ^e	-	-	0.0

^aHANSEN (1987).

^bQuartz and feldspars are combined as "non-clay detrital."

^cA dash means "not detected."

^dAll carbonate minerals are combined and reported in a single concentration value.

^eHansen does not report values for mixed-layer clays but does report concentrations for smectite (montmorillonite).

^fHansen reports mineral compositions for two samples of the Moberge Member of the Pierre Shale.

from the same core (but not necessarily the same rock material, since the concentrations of the clays, quartz, carbonates, and other minerals can range widely over short vertical distances in sedimentary rocks). Note that in the technique used in this study, it was not possible to determine the amount of amorphous material or organic compounds present, nor do the analyses include the concentrations of minerals for which there were no standards (e.g., the mineral dawsonite that is present in the Green River Formation).

Considering the nature of the difficulties in determining the absolute amounts of minerals of varying degrees of crystallinity and chemical composition (by any method), as well as the present lack of information about the amounts of amorphous and/or organic material present, the results are reasonable. Most of the differences in mineral compositions determined by QXRD can be explained on the basis of differences in the character of the samples available for analysis. In the discussions that follow, note that HANSEN (1987) combines quartz and feldspars in a single category, "non-clay" detrital, and the minerals calcite, dolomite, and siderite in a single category, "total carbonate." HANSEN (1987) does not report the presence of any mixed-layer clays, but gives concentrations for smectite.

Conasauga Group samples (CS1 and CS2) are mineralogically different from the samples analyzed by HANSEN (Table 6). This is thought to result from differences in the lithologic character of the Conasauga Group, which contains many quartz and/or calcite-rich layers. The high concentrations of calcite in samples CS1 and CS2 and the high quartz concentration in sample CS1 suggests that neither sample is a typical shale but that they are a calcareous siltstone (CS1) and, perhaps, a marlstone (CS2). The mineralogical differences are borne out by visual inspection and SEM analyses of the samples, which reveal large amounts of silt-size quartz, siliceous cement, and calcareous cement and also by their chemical compositions determined by XRF.

The Rhinestreet Shale samples are similar in composition to the single sample reported by HANSEN (1987), although DS1 and DS2 appear to contain more quartz and feldspar. Kaolinite and mixed-layer clays were identified in our samples, which are essentially carbonate free. Chlorite is present in all samples. Sample DS1 appears to be a typical shale, while DS2 might be more properly classified as a silty shale or, perhaps, as a siltstone.

The two Pierre Shale samples analyzed (PS1 and PS2) are very close in composition and their analyses (Table 6) fall within the range reported for two samples by HANSEN (1987), for example, quartz and feldspar for PS1 is 27% and for PS2 is 27%. HANSEN (1987) reports a range of 14.6 to 32.9% for non-clay detritals. Kaolinite concentrations for PS1 and PS2 are 3 and 4%, respectively; HANSEN (1987) reports a range of kaolinite concentration of 1.9 to 8.7%. The Pierre Shale contains the highest concentrations of smectites and/or mixed-layer illite/smectite clays, as well as the highest concentration of pyrite in any of the samples analyzed. Aragonite is present in both samples. The Pierre Shale is mineralogically different from the Conasauga Group samples and the Rhinestreet Shale and can be expected to behave differently from those formations. The presence of abundant pyrite in a geological material may help to maintain reducing conditions in fluids that pass through it.

The mineral concentration values for the Green River Formation samples, GR1 and GR2, agree reasonably well with those reported for a single sample (HANSEN 1987), including the total for quartz plus feldspar, and illite concentrations. The greatest differences appear to be the higher concentrations determined for dolomite and lack of information about the organics present (and rare minerals such as dawsonite). The Green River Formation is the most different of all the formations analyzed. Its clay mineral content is very small, and technically, the formation is not a shale (although locally some shale beds may be present). Thermomechanical investigations of the Green River Formation reveal the potential loss of strength (and release of volatiles) when this material is heated (HANSEN 1987).

Too few samples have been analyzed thus far to adequately state the overall precision of the technique described previously; however, it is possible to give some estimates of the precision (stated in relative error, R.E.) of some aspects of the method (MULLIGAN 1987):

1. Based on replicate analyses of the same pellet in six different orientations, the precision stated in terms of R.E. (one standard deviation) as a result of sample inhomogeneity ranges from 0.2% for quartz in a kaolinite:quartz mixture to 2.1% for quartz in an illite:quartz mixture.

2. Based on duplicate pellets prepared from the same starting material, the R.E., as a result of sample preparation, is estimated to be <3.0% (0.5% for duplicate kaolinite:quartz pellets and 3.0% for duplicate illite:quartz pellets).

3. The R.E. for taking counts on individual peaks is statistically related to the total number of counts taken. For example, if 10,000 counts are accumulated, the R.E. is 1%. If only 100 counts are accumulated, the R.E. is 10%.

4. An attempt was made to assess the R.E. as a result of measurement of peak areas using the Numonics digitizer. Two peaks, a relatively small, but sharp, quartz peak and a larger, but broader, smectite (SWal) peak were each measured ten times and the mean values and standard deviations calculated. The results were as follows:

- a. Quartz $\bar{x} = 1.30$, $S\bar{x} = 0.04$, R. E. = 3.71%; and
- b. Smectite $\bar{x} = 2.66$, $S\bar{x} = 0.02$, R. E. = 1.03%,

suggesting that the size of the peak area, rather than its shape, determines the precision of repeated measurements of an enclosed area.

3.5 PREFERRED ORIENTATION ANALYSES USING XRD

An attempt was made in this study to quantify the degree of preferred orientation of in-situ clay mineral grains in individual

sample pieces. "L-shaped" blocks were cut, trimmed, and ground (see Appendix D) to fit the available diffractometer sample holder. Each specimen was X-rayed twice, collecting intensity data for peaks lying between 2 and $62^\circ 2\theta$ for both parallel to and perpendicular to the bedding planes. At the time the data were collected, the ground surfaces were identified only by a letter "a" or "b." After the XRD patterns were run, the blocks were broken and examined to determine which surface was parallel to and which was perpendicular to the bedding. In every case, the relative intensity data for the clay peaks fit the expected pattern, i.e., the basal X-ray reflections (001) (characteristic of lattice planes parallel to the clay flakes) were enhanced relative to the (020) reflections (a set of planes essentially at 90° to the clay flakes) for the sample surface cut parallel to bedding. Examples of this contrast in intensities are shown in Fig. 1 for a sample of Rhinestreet (Devonian) Shale and Fig. 2 for a sample of Pierre Shale.

The intensity data for several samples (one block from CS2 and two blocks each from DS1, DS2, PS1, and PS2) are compared in Table 7. Data from samples CS1, GR1, and GR2 are omitted because the samples are so rich in quartz and carbonates that they do not contain sufficient quantities of clay minerals to provide useful data. An attempt is made here to compare the Rhinestreet Shale and the Pierre Shale. The ratio of the intensity of the 1.00 nm illite peak and 0.45 nm (illite plus kaolinite) peak for the Rhinestreet Shale averages 37.2 ($S\bar{x} = 7.4$), while the same ratio for the much younger (and less deeply buried) Pierre Shale averages 10.5 ($S\bar{x} = 6.3$), suggesting that the illite flakes in the Rhinestreet Shale are better oriented than those in the Pierre Shale. A similar comparison of the 0.72 nm (kaolinite) and 0.45 nm (illite plus kaolinite) peaks gives an average of 49.7 ($S\bar{x} = 19.5$) for the Rhinestreet Shale and an average of 8.4 ($S\bar{x} = 1.8$) for the Pierre Shale, also suggesting that the orientation of the kaolinite flakes is more perfect in the Rhinestreet Shale.

HANSEN (1987) reports an index of anisotropy for the Devonian Chattanooga Shale (similar to the Devonian Rhinestreet Shale)

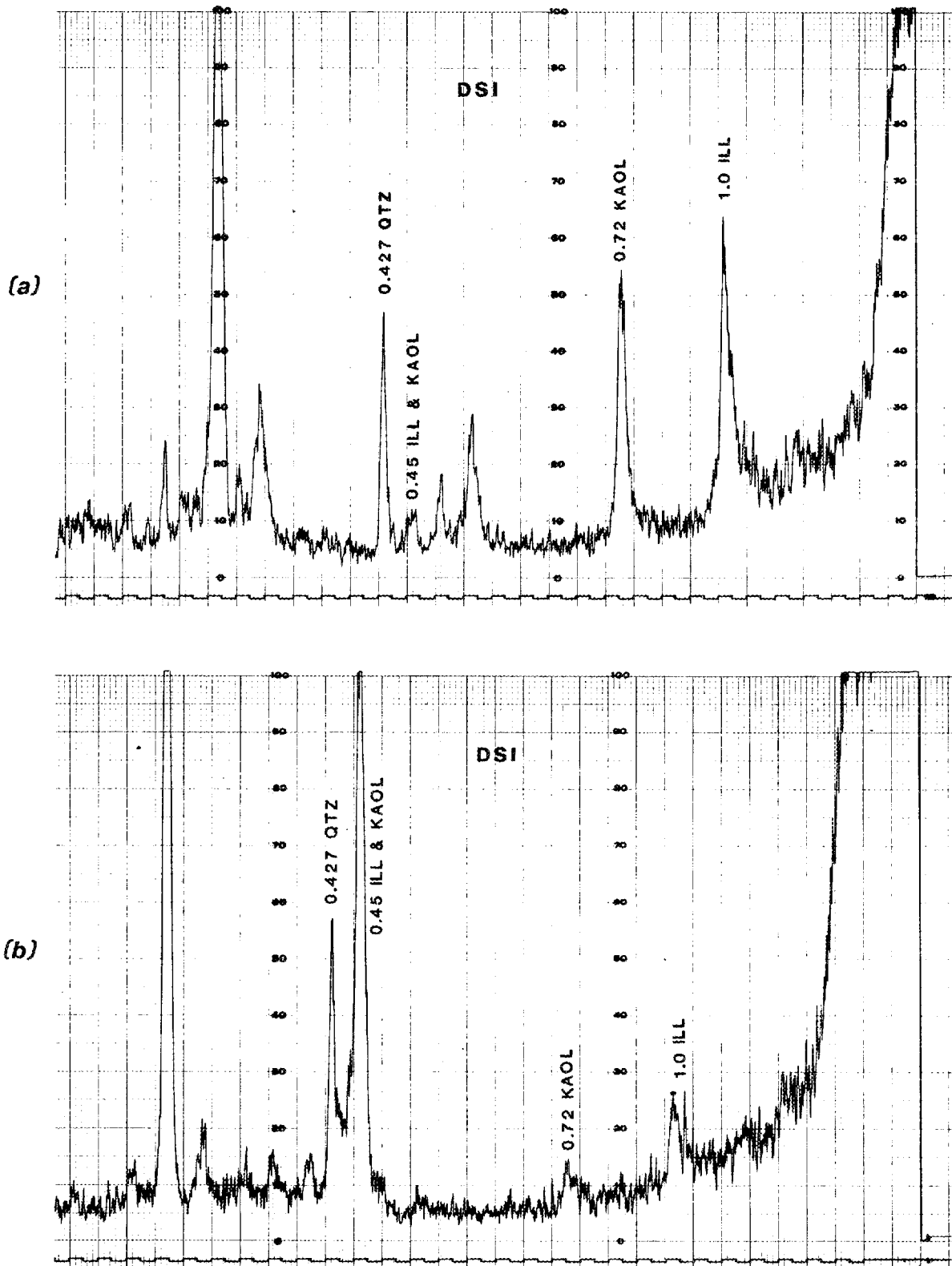


Fig. 1. X-ray diffraction patterns of samples of Devonian Shale (DS1): (a) cut essentially parallel to the bedding planes; (b) cut essentially perpendicular to the bedding planes. The illite peak is 1.00 nm (001), 0.72 nm is the (001) kaolinite peak, and 0.45 nm is the (020) peak for both illite and kaolinite.

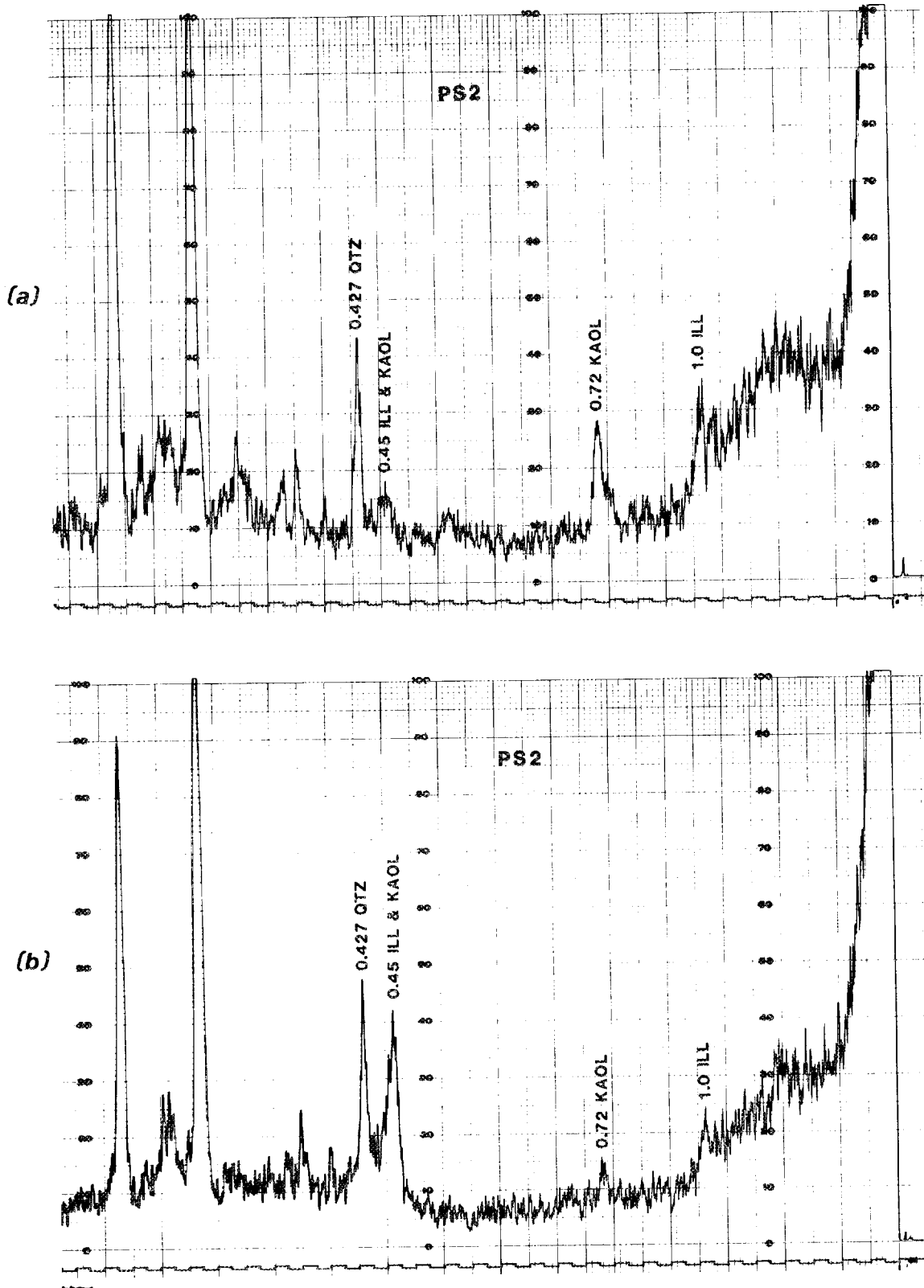


Fig. 2. X-ray diffraction patterns of samples of Pierre Shale (PS2): (a) cut essentially parallel to the bedding planes; (b) cut essentially perpendicular to the bedding planes. The illite peak is 1.00 nm (001), 0.72 nm is the (001) kaolinite peak, and 0.45 nm is the (020) peak for both illite and kaolinite.

Table 7. Results of preferred orientation study using X-ray diffraction

Sample ID number	Ratio 1.00:0.45 nm peak intensities	Ratio 0.72:0.45 nm peak intensities
CS21	14.8	38.6
DS11	43.3	71.9
DS12	28.6	a
DS21	33.5	42.2
DS22	43.4	35.1
DS ratios:	$\bar{x} = 37.2$ $S_x = 7.4$	$\bar{x} = 49.7$ $S_x = 19.5$
PS11	9.0	6.6
PS12	19.7	8.8
PS21	5.7	7.5
PS22	7.5	10.8
PS ratios:	$\bar{x} = 10.5$ $S_x = 6.3$	$\bar{x} = 8.4$ $S_x = 1.8$

^aCould not calculate this ratio because of the low intensity of one of the peaks.

of 10.5 and an index of anisotropy for the Pierre Shale of 1.8, suggesting that the mechanical strength of the Chattanooga Shale is approximately six times more anisotropic than the mechanical strength of the Pierre Shale. The X-ray intensity values obtained in this study also give higher ratios for the Rhinestreet Shale than for the Pierre Shale. Although further study is needed to confirm these results, it appears that XRD fabric analysis can be used to estimate the relative anisotropy of shale properties (mechanical, hydrologic and thermal) as a result of the degree of preferred orientation of clay mineral flakes. Material such as the Pierre Shale, with low degrees of preferred orientation, should behave in a more isotropic manner than formations such as the Rhinestreet Shale with high degrees of preferred orientation.

3.6 RESULTS OF SEM ANALYSES

SEM is an invaluable technique for studying fine-grained argillaceous material, providing several kinds of information that would be difficult to obtain by other means. Several examples are described to illustrate some of the kinds of textural, mineralogical, and chemical information that can be obtained. MULLIGAN (1987) describes additional sub-samples within the four formations examined.

Figure 3 (sample CS1, perpendicular to bedding) illustrates a relatively large (approximately 35- μm -diam.) muscovite grain, which appears to be detrital. Note the more poorly crystallized clays above and to the left of the detrital grain. Based on XRD, these are possibly mixed-layer, illite-smectite clays. To the right of and below the detrital grain, calcite (based on XRD analysis and well-developed rhombohedral cleavage) is present as an important constituent. The presence of abundant calcite cement may result in increased mechanical strength, decreased hydraulic conductivity, and decreased plasticity. The presence of abundant calcite cement may also reveal the presence of former passageways through which fluids moved.

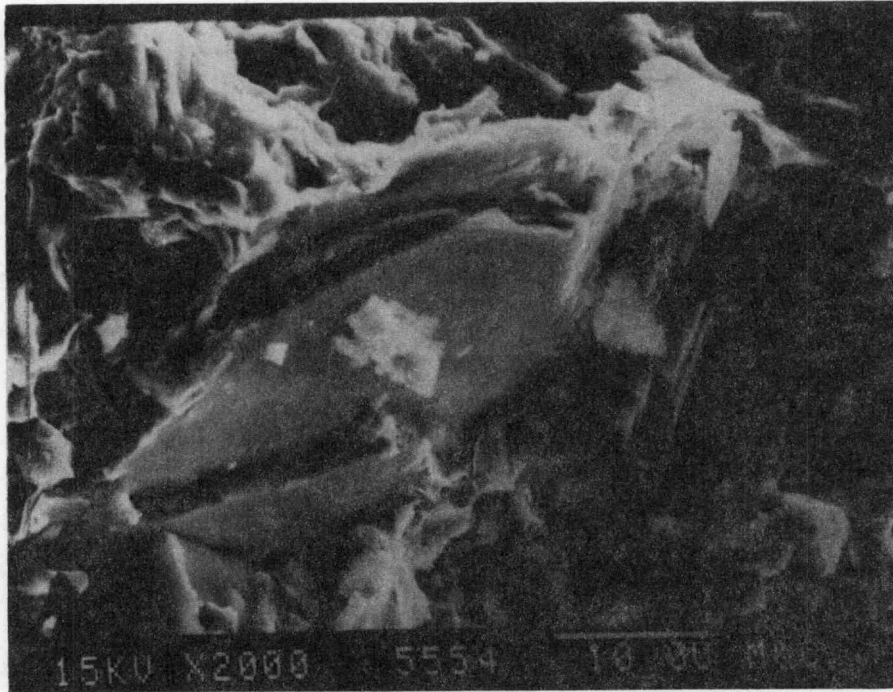


Fig. 3. SEM photograph of a relatively large detrital muscovite (illite) grain. Sample CS1, perpendicular to the bedding. A semiquantitative chemical analysis of the grain reveals the presence of Si, Al, K, Fe, and Ti.

Figure 4 (sample CS2, parallel to bedding) illustrates a silt-size detrital grain of quartz (approximately 15 μm diameter), surrounded by numerous grains of clays. The clay grains appear to be rather poorly crystallized and "wispy," and appear to be compacted or wrapped around the quartz grain. In this particular area, no calcite cement is obvious, and there may be numerous small (generally <5- μm -diam.) pores present; however, these open spaces may be an artifact of the fracturing process used to prepare the sample.

Figure 5 (sample DS2, parallel to the bedding) shows a silt-size grain of albite. Based on its anhedral shape, it is thought to be detrital rather than authigenic. It was identified on the basis of its composition, which consists primarily of Na, Al, and Si. Note the numerous grains of clay (interpreted to be primarily illite) wrapped around the feldspar grain. Many of these "clay" grains have diameters >5 μm and might be overlooked if only the clay-size fraction were analyzed using XRD. Compare these grains with the more poorly crystallized clays shown on Fig. 4 for sample CS2.

Figure 6 (sample DS2, parallel to bedding) illustrates clusters of submicrometer (framboidal?) crystals of an iron-oxide phase (the chemical analysis reveals the presence of abundant iron but no sulfur). The origin of these clusters is not known, since many of the dark-colored Devonian Shales are thought to have formed under reducing conditions, which would not favor the formation of iron oxides. Perhaps this sample came from a core taken from a depth at which groundwater could introduce dissolved oxygen, converting previously existing pyrite to iron oxides, or perhaps some pyrite was oxidized after the core was taken.

Figure 7 (sample PS2, perpendicular to bedding) shows one of numerous areas lying along bedding planes containing what appear to be secondary mineral phases. The fibrous phase appears to be either aragonite or fibrous calcite, based on its shape and major Ca in the chemical analysis, which also reveals small amounts of phosphorous and sulfur. Aragonite was detected by the XRD analyses. Minor amounts of

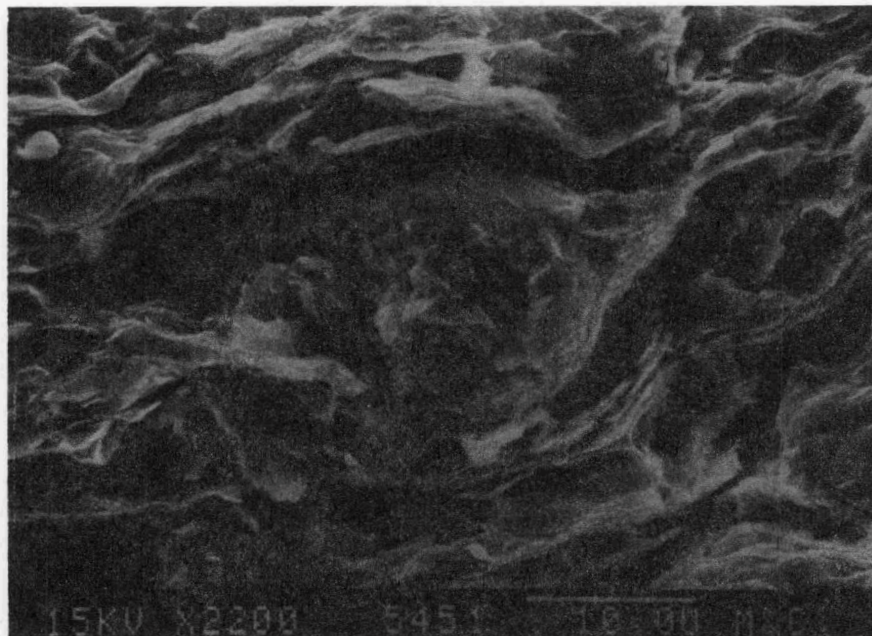


Fig. 4. SEM photograph of a silt-size, detrital quartz grain. Sample CS2, parallel to the bedding. A semiquantitative chemical analysis of the grain reveals that Si is the major element present.

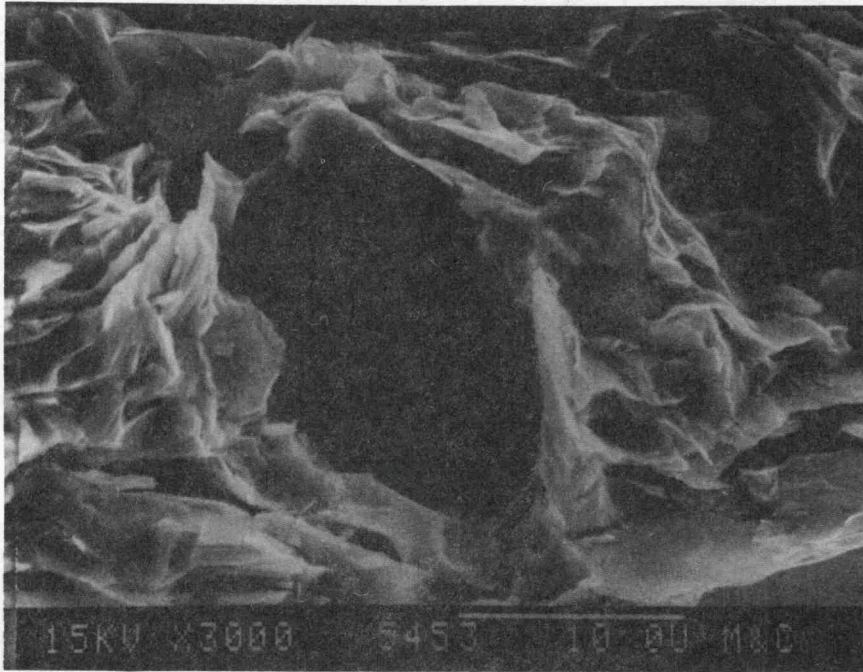


Fig. 5. SEM photograph of a silt-size, detrital albite grain. Sample DS2, parallel to the bedding. A semiquantitative chemical analysis of the grain reveals that Si, Al, and Na are the major elements present.



Fig. 6. SEM photograph of clusters of framboidal (?) iron oxide grains. Sample DS2, parallel to the bedding. A semiquantitative chemical analysis of the grains reveals that Fe is the only major element present.



Fig. 7. SEM photograph of aragonite or fibrous calcite grains. Sample PS2, perpendicular to the bedding. A semiquantitative chemical analysis of the grains reveals that Ca is the major element present with smaller amounts of P and S.

apatite and/or gypsum may be present. The Pierre Shale has a rather low specific gravity and appears to be more porous than the other shales tested. The presence of secondary phases along bedding planes suggests that fluids had passed along these openings and locally deposited new mineral phases. Whether or not fluids can still pass along such planar openings might be an important consideration in site selection.

Figure 8 (sample PS2, perpendicular to bedding) illustrates another bedding surface in the same sample as shown in Fig. 7. Note the numerous clusters of framboidal pyrite and some euhedral pyrite crystals. The deposition of pyrite along these surfaces took place under reducing conditions; hence, this material may have been formed at the time the sediments were being deposited under anoxic conditions or perhaps during diagenesis. The presence of abundant sulfides in geological material could help to maintain reducing conditions if fluids carrying radioactive wastes were later carried into them. This would help to keep the radioactive ions in less soluble valence states.

Figure 9 (sample PS2, perpendicular to bedding) shows a very large (approximately 100 μm across) biotite flake set in a matrix of very fine-grained clays and other unidentified mineral phases. Petrographic evidence, such as the well-preserved right edge, suggests that it was transported by the wind. It was probably introduced during a volcanic ash fall. Note the general lack of preferred orientation of the fine-grained matrix material.

4. FURTHER DISCUSSION AND CONCLUSIONS

Selected samples of the Conasauga Group, Rhinestreet Shale, Pierre Shale, and Green River Formation were analyzed by several techniques to determine their mineralogical compositions and to assess the effects that diagenesis may exhibit on the thermomechanical properties of these materials. Although equivalent samples were not available, eight samples (two from each formation) were selected from

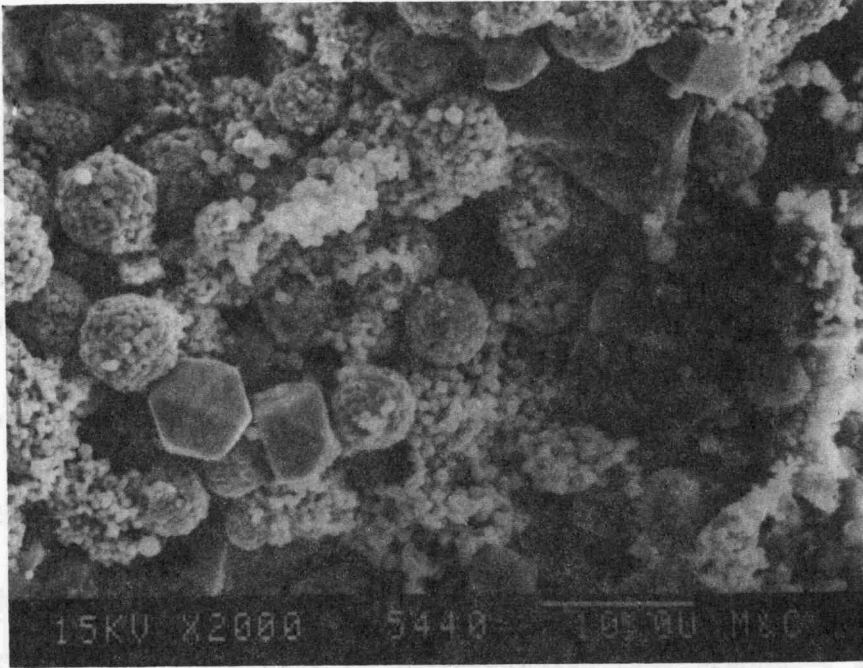


Fig. 8. SEM photograph of framboidal and euhedral pyrite grains. Sample PS2, perpendicular to the bedding. A semiquantitative chemical analysis of the grains reveals that Fe and S are the major elements present.

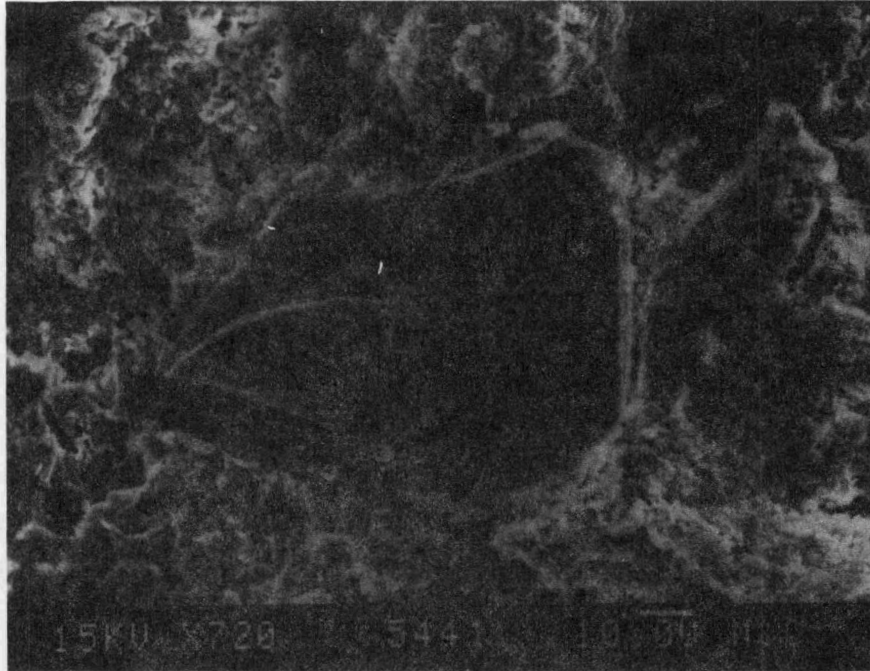


Fig. 9. SEM photograph of a relatively large, possibly wind-blown grain of biotite. Sample PS2, perpendicular to the bedding. A semiquantitative chemical analysis of the grain reveals that Si, Al, K, Mg, Fe, and Ti are present.

the same suite of cores from which samples for thermomechanical tests had been chosen.

Mineral concentrations for Pierre Shale and Green River Formation samples are in agreement with the ranges of values obtained for samples of those formations by HANSEN (1987). The samples for which there were the greatest differences in mineralogical composition came from the Conasauga Group.

The results of thermomechanical tests for the Rhinestreet Shale, Pierre Shale, and Green River Formation show that the average ultimate strengths of these formations range from 7.2 MPa for the Pierre Shale to 94.8 MPa for the Green River Formation. Attempts to relate the information obtained in the study with the data on ultimate strength (HANSEN 1987) should be made with caution. The ultimate strength of the Green River Formation may be a result of its high concentration of dolomite and calcite, which act like cement to hold individual mineral grains together, or it could be attributed to the presence of organic compounds in pore space. Note that the average ultimate strength of the Rhinestreet Shale increases from 58.7 MPa at room temperature to 74.7 MPa at 150°C (because of the loss of minor pore fluids present, according to HANSEN 1987), while that of the Green River Formation decreases to 24.7 MPa, which is thought to result from the softening and volatilization of organic compounds present (HANSEN 1987). The lower ultimate strength of the Pierre Shale compared with that of the Rhinestreet Shale is thought to be a result of its higher water content and the presence of very fine-grained, mixed-layer clays and smectites in the Pierre Shale. Several studies cited by MEYER (1983) illustrate the role of water and smectite in lowering strength properties in laboratory samples. The Pierre contains the highest concentration of smectites and/or mixed-layer clay minerals and the highest concentration of pyrite among the samples analyzed. SEM observations reveal mineral matter (such as aragonite and pyrite) along the bedding planes of the Pierre Shale samples.

Preferred orientation analysis of the Rhinestreet Shale, using XRD, suggests that its mechanical properties will depend on whether the property is measured parallel to or perpendicular to the bedding direction of the sample. Properties that may be influenced by the degree of preferred orientation of clay flakes (e.g., mechanical strength, hydraulic conductivity, and thermal conductivity) should be less affected by orientation in the Pierre Shale than in formations such as the Rhinestreet Shale with its high degree of preferred orientation.

The Pierre Shale is mechanically weak (average ultimate strength 7.2 MPa) and may be subject to swelling or shrinking depending on the conditions of temperature and humidity. HANSEN (1987) reports that the slake durability of the Pierre Shale (19 tests) ranged from "low to medium" while the Rhinestreet Shale (three tests) and the Green River Formation (three tests) both ranked "extremely high." The lack of durability of the Pierre Shale is due to its lack of compaction and cementation (as shown by its high porosity and low specific gravity), as well as its smectite and mixed-layer clay content. Smectite and/or mixed-layer clays (approximately 26 wt % in one of the Pierre Shale samples analyzed) may release water if they are thermally loaded because of the radiogenic heat.

The Green River Formation is mineralogically and lithologically the most different from the other formations tested. Its clay mineral content is <5%, and it is dominated by dolomite and calcite. Thermomechanical testing of the Green River Formation reveals the potential loss of strength (and release of volatiles) when this material rich in organic matter is heated.

In general, QXRD can be an important source of information concerning any clay-rich material that might be considered as hosts, buffer, or backfill material for the geological disposal of high-level radioactive waste. The kinds and amounts of clay minerals present, as well as the presence of other minerals such as zeolites and sulfides,

will influence the sorption coefficients and oxidation-reduction behavior of these formations. The results of QXRD should be combined with other methods, such as preferred orientation analysis and SEM analysis, which can provide information concerning grain sizes and size distribution, grain shapes and orientations, and the presence of cements and their mineralogical characteristics.

REFERENCES

- BURST 1982. J. F. Burst, "Diagenesis of Gulf Coast Clayey Sediments and Its Possible Relation to Petroleum Migration," Amer. Assoc. Petrol. Geol. Bull., 53, 73-93 (1982).
- CHUNG 1974a. F. W. Chung, "Quantitative Interpretation of X-ray Diffraction Patterns of Mixtures. I. Matrix Flushing Method for Quantitative Multi-component Analysis," J. Appl. Cryst., 7, 519-525 (1974).
- CHUNG 1974b. F. W. Chung, "Quantitative Interpretation of X-ray Diffraction Patterns of Mixtures. II. Adiabatic Principle of X-ray Diffraction Analysis of Mixtures," J. Appl. Cryst., 7, 526-531 (1974).
- CROFF, in preparation. A. G. Croff, T. F. Lomenick, R. S. Lowrie, and S. H. Stow, Evaluation of Five Sedimentary Rocks Other than Salt for Geologic Repository Siting. V.1. Main Report and Appendixes A and B, ORNL-6241/V1, Oak Ridge National Laboratory.
- DAVIS 1982. B. L. Davis and L. R. Johnson, "Sample Preparation and Methodology for X-ray Quantitative Analysis of Thin Aerosol Layers Deposited on Glass Fiber and Membrane Filters," Advances in X-ray Analysis, Vol. 25, Plenum Press, 1982.
- DAVIS 1984. B. L. Davis, "Reference Intensity Quantitative Analysis Using Thin-Layer Aerosol Samples," Advances in X-ray Analysis, Vol. 27, Plenum Press, 1984.
- DAVIS 1987. B. L. Davis, "Quantitative Determination of Mineral Content of Geological Samples by X-ray Diffraction: Discussion," Amer. Mineral., 72, 438-440 (1987).
- DELAGUNA 1968. W. DeLaguna, Engineering Development of Hydraulic Fracturing as a Method for Permanent Disposal of Radioactive Waste, ORNL-4259, Oak Ridge National Laboratory, 1968.
- GRIFFIN 1970. G. M. Griffin, "Interpretation of X-ray Diffraction Data," in Procedures of Sedimentary Petrology, R. E. Carver, ed., Wiley Interscience, New York, 1970.
- HANSEN 1987. F. D. Hansen and T. J. Vogt, Thermomechanical Properties of Selected Shales, ORNL/Sub/85-97343/2 (RSI-0305), Oak Ridge National Laboratory, 1987.
- KOPP 1986. O. C. Kopp, A Preliminary Assessment of Mineralogical Criteria on the Utility of Argillaceous Rocks and Minerals for High-Level Radioactive Waste Disposal, ORNL/TM-9979, Oak Ridge National Laboratory, 1986.

- KOPP 1987. O. C. Kopp, "Mineralogical Control of Chemical and Hydrologic Properties of Sedimentary Rock Geological Repositories," GSA Abstracts with Programs, Vol. 19, No. 7, 732, 1987.
- MEYER 1983. D. Meyer and J. J. Howard, Evaluation of Clays and Clay Minerals for Application to Repository Sealing, ONWI-486, 1983.
- MONGER 1986. H. C. Monger, Geochemical and Mineralogical Properties of Copper Ridge and Chapultepec Regolith at the Oak Ridge National Laboratory Reservation - West Chestnut Ridge Site, Unpublished Master's Thesis, University of Tennessee, 112 pp, 1986.
- MULLIGAN 1987. P. J. Mulligan, Quantitative Mineralogical Analysis and Scanning Electron Microscopy Techniques for the Study of Argillaceous Formations Which are Potential Candidates for the Geologic Disposal of High-Level Radioactive Waste, Unpublished Master's Thesis, University of Tennessee, 109 pp, 1987.
- PAWLOWSKI 1985. G. A. Pawlowski, "Quantitative Determination of Mineral Content of Geological Samples by X-ray Diffraction," Amer. Mineral., 70, 663-337 (1985).
- PAWLOWSKI 1987. G. A. Pawlowski, "Quantitative Determination of Mineral Content of Geological Samples by X-ray Diffraction: Reply," Amer. Mineral., 72, 441-443 (1987).
- POTTER 1980. P. E. Potter, J. B. Maynard, and W. A. Pryor, Sedimentology of Shale, Springer-Verlag, New York, 1980.
- RIEKE 1974. H. H. Rieke and G. V. Chilingarian, Compaction of Argillaceous Sediments, Development in Sedimentology, Vol. 16, 1974.
- SHAW 1954. D. B. Shaw and C. E. Weaver, "The Mineralogical Composition of Shales," J. Sed. Petrol., 35, 213-222 (1965).
- WEAVER 1976. C. E. Weaver, Thermal Properties of Clays and Shales, Y/OWI/Sub-7009-1, Office of Waste Isolation, Union Carbide Nuclear Division, Oak Ridge, Tennessee, 1976.

6. APPENDIXES

Appendix A

PROCEDURE FOR THE DETERMINATION OF SPECIFIC GRAVITIES OF SHALES
AND OTHER FRAGILE OR POROUS MATERIAL

1. Select a sample of the material to be tested that is free from loose surface material, jagged edges, indentations, etc. The sample should weigh at least 5 g and, in general, less than 50 g for convenience in handling.
2. Weigh the sample to the nearest 0.01 to 0.001 g. (In most cases, weighing to 0.01 g is sufficient because other sources of small errors, e.g., loss of sample while handling with forceps, trapped air at the surface, etc., are likely to keep the precision of the determination to ± 0.01 units of specific gravity.)
3. Using forceps, dip one end of the sample into molten paraffin (M.P. approximately 60°C). It may have to be dipped a few times to get a thin coating on the end. After the paraffin has cooled, turn the sample around and dip the other end to get it completely enclosed.
4. Re-weigh the paraffin-coated sample and determine the mass of the paraffin by difference.
5. If the specific gravity of the paraffin is not known, it may be determined by measuring its weight loss in ethanol (S.G. = 0.7893) or methanol (S.G. = 0.7914). Paraffin usually has an S.G. in the range of 0.896 to 0.925. The S.G. of the paraffin used in our tests is 0.902 (density = 0.902 g/cm³).
6. Determine the volume (in cubic centimeters) of the paraffin coating, using the relationship:

$$\text{Volume (cm}^3\text{)} = \text{Mass (g)}/\text{Density (g/cm}^3\text{)}$$

7. Using a standard specific-gravity balance, determine the weight loss of the paraffin-coated sample in distilled water at 20°C. The weight loss (in grams) is due to the volume of the displaced

water and, hence, the volume (in cubic centimeters) of the sample and its paraffin coating.

8. Subtract the volume of the paraffin coating previously determined (step 6) from the volume of the coated sample. The difference is equal to the original volume of the uncoated sample.
9. The specific gravity of the uncoated sample can be quickly determined by dividing the mass of the original, uncoated sample (in grams) by the volume (in cubic centimeters) of the uncoated sample determined in step 8. In effect, the mass and volume of the paraffin coating have been removed. The only function of the coating is to protect the sample from penetration by the water or slaking.

APPENDIX B

Appendix B

INFORMATION CONCERNING THE X-RAY FLUORESCENCE ANALYSIS

Table B.1. Analytical conditions

Condition	KV	μ A	Filter	Anode	Elements
1	10.0	150	Open	Rh	Na ₂ O, MgO, Al ₂ O ₃ , SiO ₂ , P ₂ O ₅ , S, K ₂ O, CaO
2	30.0	250	Cu	W	TiO ₂ , Cr, MnO, Fe ₂ O ₃
3	45.0	175	In	W	Ba
4	40.0	175	In	W	Rb, Sr, Zr

Table B.2. Calibration range of standards and standard errors of calibration

Element or oxide	Range (wt %)	Standard error ^a
Na ₂ O	0.08 - 10.40	0.24
MgO	0.04 - 4.50	0.16
Al ₂ O ₃	5.76 - 20.64	0.21
SiO ₂	28.29 - 68.46	0.29
P ₂ O ₅	0.097 - 0.687	0.009
S	0.010 - 1.89	0.009
K ₂ O	1.04 - 11.20	0.05
CaO	0.12 - 20.71	0.07
TiO ₂	0.010 - 1.61	0.023
Cr	0.0016 - 0.0438	0.0041
MnO	0.0023 - 0.1149	0.0083
Fe ₂ O ₃	0.10 - 8.58	0.10
Ba	0.0112 - 0.1800	0.0082
Rb	0.0035 - 0.0368	0.0010
Sr	0.0055 - 0.0445	0.0013
Zr	0.0059 - 0.0790	0.0014

^aIn weight percent (one standard deviation).

Table B.3. Replicate analyses of standards analyzed as unknowns

Element	Sample DKTS		Sample SC01	
	Calculated value %	STD value %	Calculated value %	STD value %
Na ₂ O	0.27	0.23	0.49	0.83
MgO	1.86	1.86	2.36	2.40
Al ₂ O ₃	15.96	16.07	13.65	13.96
SiO ₂	61.60	62.85	60.66	62.75
P ₂ O ₅	0.28	0.29	0.17	0.19
S	0.04	0.02	0.08	0.07
K ₂ O	4.81	4.87	2.62	2.65
CaO	0.12	0.14	2.55	2.58
TiO ₂	0.70	0.71	0.60	0.61
Cr	0.0267	0.0267	0.0095	0.0093
MnO	0.0475	0.0471	0.0618	0.0610
Fe ₂ O ₃	7.33	7.45	5.09	5.14
Ba	0.1992	0.1754	0.0661	0.0601
Rb	0.0242	0.0234	0.0125	0.0120
Sr	0.0098	0.0101	0.0181	0.0183
Zr	0.0269	0.0278	0.0184	0.0178

Element	Sample SGR1		Sample S02	
	Calculated value %	STD value %	Calculated value %	STD value %
Na ₂ O	2.35	2.48	2.51	2.55
MgO	4.37	4.49	1.00	1.03
Al ₂ O ₃	6.96	7.24	15.38	15.27
SiO ₂	27.26	28.28	52.69	53.43
P ₂ O ₅	0.28	0.30	0.68	0.68
S	1.89	1.89	0.03	0.02
K ₂ O	1.70	1.72	2.38	2.39
CaO	8.82	8.88	2.73	2.74
TiO ₂	0.35	0.34	1.41	1.43
Cr	0.0066	0.0056	0.0057	0.0051
MnO	0.0485	0.0485	0.0934	0.0942
Fe ₂ O ₃	3.58	3.65	7.79	7.88
Ba	0.0609	0.0416	0.1230	0.1107
Rb	0.0093	0.0091	0.0065	0.0072
Sr	0.0450	0.0450	0.0346	0.0343
Zr	0.0056	0.0056	0.0810	0.0790

APPENDIX C

Appendix C

CHEMICAL COMPOSITIONS OF SAMPLES

Element	Sample CS1 calculated value %	Sample CS2 calculated value %
Na ₂ O	2.00	2.15
MgO	2.35	2.33
Al ₂ O ₃	7.76	14.37
SiO ₂	46.63	49.46
P ₂ O ₅	0.22	0.31
S	0.12	0.54
K ₂ O	1.91	3.00
CaO	14.78	10.53
TiO ₂	0.37	0.61
Cr	0.0016	0.0070
MnO	0.1465	0.1571
Fe ₂ O ₃	2.90	4.46
Ba	N.D. ^a	N.D. ^a
Rb	0.0043	0.0085
Sr	0.0233	0.0210
Zr	0.0223	0.0236

Element	Sample DS1 calculated value %	Sample DS2 calculated value %	Sample CHAT1 calculated value %
Na ₂ O	1.29	1.32	2.19
MgO	1.85	1.66	2.17
Al ₂ O ₃	23.97	21.33	12.47
SiO ₂	57.94	60.58	44.48
P ₂ O ₅	0.38	0.17	1.08
S	1.86	0.25	8.80
K ₂ O	4.62	4.63	2.13
CaO	0.26	0.36	N.D. ^a
TiO ₂	0.96	0.87	0.7624
Cr	0.0107	0.0104	0.0043
MnO	0.0344	0.0482	0.0246
Fe ₂ O ₃	7.11	5.54	9.96
Ba	0.0703	0.0484	N.D. ^a
Rb	0.0237	0.0231	0.0114
Sr	0.0163	0.0144	0.0086
Zr	0.0153	0.0146	0.0281

^aNot determined.

Appendix C
(continued)

Element	Sample PS1 calculated value %	Sample PS2 calculated value %
Na ₂ O	1.45	1.81
MgO	2.37	2.11
Al ₂ O ₃	14.65	15.50
SiO ₂	47.56	48.66
P ₂ O ₅	0.40	0.62
S	1.07	2.08
K ₂ O	2.39	2.17
CaO	6.50	6.29
TiO ₂	0.60	0.59
Cr	0.0099	0.0098
MnO	0.0914	0.0476
Fe ₂ O ₃	6.95	5.71
Ba	0.0300	0.0346
Rb	0.0093	0.0086
Sr	0.0291	0.0313
Zr	0.0139	0.0135

Element	Sample GR1 calculated value %	Sample GR2 calculated value %
Na ₂ O	1.85	1.55
MgO	4.74	4.55
Al ₂ O ₃	5.78	6.46
SiO ₂	25.57	27.84
P ₂ O ₅	0.27	0.72
S	0.47	0.94
K ₂ O	1.10	0.85
CaO	17.48	9.98
TiO ₂	0.28	0.31
Cr	0.0005	0.0032
MnO	0.0442	0.0416
Fe ₂ O ₃	1.97	2.26
Ba	0.0368	0.0418
Rb	0.0036	0.0054
Sr	0.0857	0.0800
Zr	0.0005	0.0011

APPENDIX D

Appendix D
PREPARATION OF "L-SHAPED" BLOCKS

L-shaped blocks were cut from shale fragments that were approximately 3.5 to 5 cm in diameter (or along an edge). Two intersecting planes, one essentially parallel to the most obvious bedding or lamination planes and the second at 90° to the first, were chosen and marked. Two surfaces were cut along these planes, using an SiC-impregnated cutting wheel. The remainder of the block was then trimmed into a rectangular block approximately 1.5 cm x 1.5 cm x 2 cm along its edges. Two additional cuts were made below the "parallel to bedding" and "perpendicular to bedding" surfaces formed by the first two cuts, approximately 0.6 cm below the surface, forming an L-shaped block (Fig. D-1).

ORNL DWG 88-1214

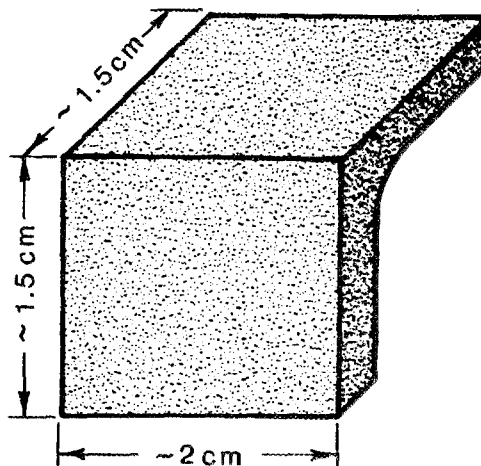


Fig. D-1. Sketch of fabricated "L-shaped" block.

The rough, sawed surfaces were ground (dry) on emery grinding papers, using successively finer papers down to #320 grit (very fine) backed by a flat glass plate to remove surface material that may have been damaged by heat during the sawing process and saw marks. During the trimming and grinding process, the bedding plane features used to keep track of the orientations of the surfaces to be X-rayed were

sometimes masked; however, before the samples were X-rayed, each surface was given an identifying letter. After the intensity data were obtained, the block was broken so that the position of the bedding planes could be positively determined. In every case, the X-ray intensity data for (00 l) reflections were enhanced for the plane cut essentially parallel to the bedding.

Note that the blocks used in this preliminary study were cut, trimmed, and ground using hand-held tools. When the blocks were broken open, it was noted that, in some cases, the final surfaces were off by perhaps as much as 5° from the desired directions. If the information obtained by this technique should prove to be valuable, the procedure could be improved significantly by using machine tools. As a first approximation, the hand-cut samples revealed large differences in the intensities of clay mineral peaks, which appear to be directly related to the degree of preferred orientation of the clay mineral flakes in the sample.

INTERNAL DISTRIBUTION

- | | |
|-----------------------|---------------------------------|
| 1. W. D. Arnold | 24. J. D. Marsh |
| 2. G. Cowart | 25. R. E. Mesmer |
| 3. A. G. Croff | 26. R. E. Meyer |
| 4. R. B. Dreier | 27. E. Peelle |
| 5. L. M. Ferris | 28. D. E. Reichle |
| 6. V. T. Hinkel | 29-30. S. H. Stow |
| 7. R. G. Genung | 31. V. S. Tripathi |
| 8. P. C. Ho | 32. K. L. Von Damm |
| 9. L. K. Hyder | 33. G. T. Yeh |
| 10. G. K. Jacobs | 34. Central Research Library |
| 11-15. O. C. Kopp | 35. Document Reference Section |
| 16. Z. S. Kooner | 36-37. Laboratory Records |
| 17. R. L. Jolley | 38. Laboratory Records, ORNL/RC |
| 18. S. Y. Lee | 39. ORNL Patent Office |
| 19-23. T. F. Lomenick | 40. ORNL Y-12 Technical Library |

EXTERNAL DISTRIBUTION

41. DOE/ORO, Office of Assistant Manager for Energy Research and Development, P. O. Box 2001, Oak Ridge, TN 37831

Department of Energy, Office of Civilian Radioactive Waste Management, 1000 Independence Avenue SW, Washington, DC 20585

- | | |
|-------------------|------------------|
| 42. D. Alexander | 51. S. Gomberg |
| 43. I. Alterman | 52. C. Hanlon |
| 44. R. Blaney | 53. J. Kimball |
| 45. S. J. Brocoum | 54. K. Mihm |
| 46. R. Cady | 55. M. Mozumder |
| 47. N. Eisenberg | 56. S. Singal |
| 48. G. Faulkner | 57. R. Wallace |
| 49. M. Frei | 58. D. Youngberg |
| 50. B. Gale | |

Department of Energy, Chicago Operations Office, 9800 S. Cass Avenue, Chicago, IL 60439

- | | |
|----------------------|------------------|
| 59. R. Baker | 62. E. Paterna |
| 60. A. Bendokis | 63. R. Rothman |
| 61. J. D. Kasprowicz | 64. H. W. Smedes |

Department of Energy, Nevada Operations

- | | |
|------------------|-------------------|
| 65. M. Blanchard | 67. D. Livingston |
| 66. R. Levich | 68. H. Ahagen |

Battelle Memorial Institute, Office of Waste Technology Development,
Battelle Project Management Division, 7000 S. Adams St., Willowbrook,
IL 60521

- | | |
|-----------------|------------------|
| 69. W. Newcomb | 72. G. Stirewalt |
| 70. R. Laughon | 73. A. Yonk |
| 71. R. Robinson | |

Earth Sciences Division, Lawrence Berkeley Laboratory, One Cyclotron
Road, Berkeley, CA 94720

- 74. J. Long
- 75. L. Myer
- 76. P. A. Witherspoon

Re/Spec, Inc., P. O. Box 725, Rapid City, SD 57701

- 77. A. Fossum
- 78. P. F. Gnirk

Center for Tectonophysics, Texas A&M University, College Station, TX 77843

- 79. P. A. Domenico
- 80. J. E. Russell

Roy F. Weston, Inc., 2301 Research Blvd., Rockville, MD 20850

- | | |
|-------------------|----------------|
| 81. M. K. Cline | 84. D. Siefken |
| 82. K. Czyscinski | 85. W. Wowak |
| 83. R. E. Jackson | |

Los Alamos Scientific Laboratory, P. O. Box 1663, Los Alamos, NM 87545

- 86. J. Canepa
- 87. B. Crowe
- 88. R. Aines, Lawrence Livermore National Laboratory, P. O. Box 808,
Livermore, CA 94550
- 89. D. G. Brookins, 3410 Groman Court, Albuquerque, NM 87110
- 90. N. H. Cutshall, Johnson Associates, 10461 White Granite Dr., Suite
204, Oakton, VA 22124
- 91. F. A. Donath, The Earth Technology Corp., 3777 Long Beach Blvd.,
Long Beach, CA 90807
- 92. Serge Gonzales, Earth Resource Associates, Inc., 295 E. Dougherty
St., Suite 105, Athens, GA 30601

93. K. S. Johnson, Earth Resource Associates, 1321 Greenbriar Dr., Norman, OK 73069
94. B. Y. Kanehiro, Berkeley Hydrotechnique, Inc., 2150 Shattuck Ave., Berkeley, CA 94704
95. Emil Kowalski, Division Head, Repository Projects, NAGRA, Parkstrasse 23, CH-5401, Baden, Switzerland
96. T. Pigford, Department of Nuclear Engineering, College of Engineering, University of California, Berkeley, CA 94720
97. Paul Potter, Department of Geology, University of Cincinnati, Cincinnati, OH 45221
98. K. Sugihara, Power Reactor and Nuclear Fuel Development Corp., 9-13 1-Chome Akasaka, Minato-Ku, Tokyo, Japan
99. Ming-Kuan Tu, Central Geological Survey, Box 968, Taipei, Taiwan, Republic of China
100. Frank J. Wobber, Ecological Research Division, Office of Health and Environmental Research, Office of Energy Research, MS-E201, Department of Energy, Washington, DC 20545
101. P. J. Mulligan, Department of Geological Sciences, University of Tennessee, Knoxville, TN 37996-1410
102. D. K. Reeves, Department of Geological Sciences, University of Tennessee, Knoxville, TN 37996-1410
- 103-112. Office of Scientific and Technical Information, P. O. Box 62, Oak Ridge, TN 37830